Iron(III)−Hydrogen Peroxide Reaction: Kinetic Evidence of a Hydroxyl-Mediated Chain Mechanism

Joaquin F. Perez-Benito*

Departamento de Quimica Fisica, Facultad de Quimica, Universidad de Barcelona, Marti i Franques 1, 08028 Barcelona, Spain

Received: December 17, 2003; In Final Form: March 23, 2004

The kinetics of decomposition of H_2O_2 catalyzed by Fe^{3+} in aqueous solution in the presence of HNO_3 has been followed by permanganate titration and studied by the initial-rate method. In the experimental range $[H_2O_2]_0/[Fe^{3+}] = 41-2028$ used in this study, the initial rate follows the law $v_0 = \{k([Fe^{3+}]^{3/2}[H_2O_2]_0^{1/2})/([H^+]^{3/2})\}/\{(1 + k'([Fe^{3+}]/([H_2O_2]_0[H^+])))^{1/2}\}$. Both rate constants k and k' decrease with increasing ionic strength, and the corresponding apparent activation energies are 146 ± 10 and 88 ± 21 kJ mol^{-1}. The experimental rate law strongly suggests a radical-chain mechanism, with Fe^{2+}, $HO^{\bullet}$, $HO_2^{\bullet}$, and $O_2^{\bullet-}$ as propagating intermediates. At high values of the $[H_2O_2]_0/[Fe^{3+}]$ ratio two different reactions compete as chain-termination steps (dismutation of $HO_2^{\bullet}$ radicals and reduction of $HO_2^{\bullet}$ by Fe^{2+}), whereas at lower values of that ratio a third chain-termination step (reduction of $HO^{\bullet}$ by Fe^{2+}) also contributes. Thus, the kinetics of this reaction can be considered as an indirect proof of the participation of hydroxyl radicals in the mechanism.

Introduction

It has often been proposed that some transition-metal ions in their lower oxidation states are capable of reducing hydrogen peroxide with the formation of a hydroxyl free radical.[1−3] The most famous case is probably the Fenton reaction, with Fe(II) as the reducing agent.[4−6] However, there exist strong discrepancies on the actual formation of a hydroxyl radical from that reaction.[7−19] Direct identification of this intermediate in the Fe(III)−H_2O_2 and Fe(II)−H_2O_2 reactions has so far proven to be elusive; for instance, the use of spin-trap reagents has not yielded conclusive results.[20]

Although some authors have interpreted their kinetic results on the Fe(III)−H_2O_2 reaction in terms of a radical-chain mechanism,[21,22] a definitive proof has never been provided, and other authors have favored nonradical mechanisms.[23,24] In early studies of the reaction in acidic solution, the rate law found was

$$v = k_s\frac{[Fe^{3+}][H_2O_2]}{[H^+]} \qquad (1)$$

Unfortunately, it has been pointed out that such a simple rate law is compatible with a number of different mechanisms, involving free radicals as intermediates or not.[25] However, posterior kinetic studies reported the existence of some deviations with respect to that basic rate law.[26,27]

Now, I present the results of a kinetic study leading to a different rate law. The new law is much more complex than eq 1, although it reduces to eq 1 under some experimental conditions. However, the differences between the two laws are very important, since they greatly reduce the number of possible mechanisms. The new rate law strongly suggests that the decomposition of H_2O_2 catalyzed by Fe(III) is a free-radical chain reaction, and it beautifully fits a hydroxyl-radical-mediated mechanism. This mechanism easily accommodates not only the experimental data found in this work but also those reported by other authors under different experimental conditions.

Experimental Section

The solvent was water previously purified by deionization, distillation, and circulation through a Millipore system. Hydrogen peroxide (30% additive-free aqueous solution), $FeCl_3{\cdot}6H_2O$, and HNO_3 (65% aqueous solution) were obtained from Fluka and KNO_3 from Merck.

Air-saturated solutions were used in the kinetic experiments. The reaction was followed by taking aliquots from the thermostated reacting mixture at appropriate intervals and titrating them with potassium permanganate in the presence of excess sulfuric acid.[28] To quench the Fe(III)−H_2O_2 reaction, an appropriate volume (approximately 40 mL) of $KMnO_4$ (1.00×10^{-2} M) was rapidly added from the buret to 20 mL of H_2SO_4 (0.711 M); then the reacting-mixture aliquot (typically 4 mL) was also added, and after homogenization, more $KMnO_4$ solution (approximately 1 mL) was slowly added from the buret until all the H_2O_2 was consumed. A Brand Bürette Digital II (accuracy ±0.01 mL) was used for the titrations.

Results

Kinetic Method. The kinetic data were obtained using the initial-rate method. The reaction follows the stoichiometry[26]

$$2H_2O_2 = 2H_2O + O_2 \qquad (2)$$

The first stretch (typically, up to 2−10% of H_2O_2 conversion) of each kinetic run (Figure 1) was fitted to the approximate equation

$$\ln [H_2O_2] = a_0 + a_1 t \qquad (3)$$

and the initial rate was obtained as

$$v_0 = -\frac{1}{2}\left(\frac{d[H_2O_2]}{dt}\right)_{t=0} = -\frac{1}{2}a_1[H_2O_2]_0 \qquad (4)$$

* Fax: 34 93 4021231. E-mail: j.perez@qf.ub.es.

10.1021/jp031339l CCC: $27.50
Published on Web 05/07/2004

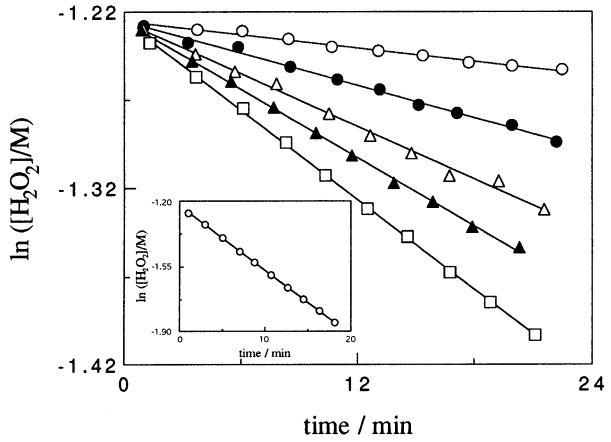

Figure 1. Kinetic plots for the iron(III)-catalyzed decomposition of H_2O_2 (0.294 M) in the presence of HNO_3 (2.31×10^{-2} M) at 25.0 °C: $[FeCl_3] = 0.48$ (○), 0.97 (●), 1.45 (△), 1.93 (▲), and 2.41 (□) $\times 10^{-3}$ M. The inset shows the kinetic plot for the decomposition of H_2O_2 (0.294 M) catalyzed by $FeCl_3$ (2.41×10^{-3} M) in the presence of HNO_3 (2.31×10^{-2} M) at 35.0 °C.

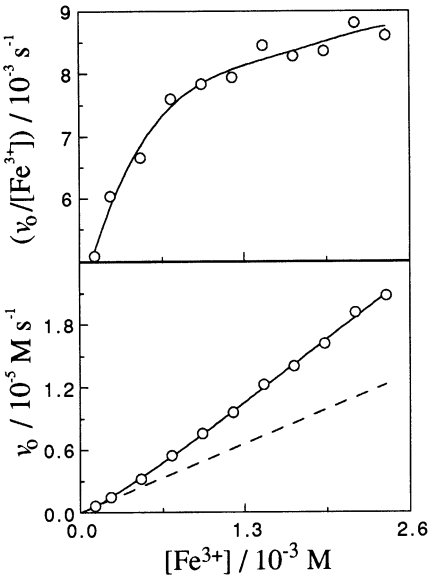

Figure 2. Dependence of the initial rate (bottom) and the $v_0/[Fe^{3+}]$ ratio (top) on the catalyst concentration for the iron(III)-catalyzed decomposition of H_2O_2 (0.294 M) in the presence of HNO_3 (2.31×10^{-2} M) at 25.0 °C. The dashed line represents the tangent to the curve at [catalyst] = 0.

At high values of $[Fe^{3+}]$, the ln $[H_2O_2]$ vs t plots showed a good linearity for at least one half-life (Figure 1, inset). All the experiments were duplicated. The total number of kinetic runs was 396, 10 aliquots were titrated in each kinetic run, and the typical reproducibility of the initial rate was within ±2%.

Apparent Kinetic Orders. The v_0 vs $[Fe^{3+}]$ plots were roughly linear; although high linear correlation coefficients (>0.999) were obtained for them, the intercepts were invariably negative, and at high catalyst concentrations, the initial rate was much higher than expected from the tangent to the curve at $[Fe^{3+}] = 0$ (Figure 2, bottom). The discrepancies with the predictions of eq 1 were even more evident when the $v_0/[Fe^{3+}]$ ratio was plotted against the catalyst concentration. If the reaction rate was first-order dependent on $[Fe^{3+}]$, the $v_0/[Fe^{3+}]$ vs $[Fe^{3+}]$ plots should lead to horizontal straight lines, but clear-cut increasing curves were obtained instead (Figure 2, top). Thus, the apparent order of the catalyst is >1.

TABLE 1: Apparent Kinetic Orders of Hydrogen Peroxide and Hydrogen Ion at Various Iron(III) Concentrations[a]

$[Fe^{3+}]/10^{-3}$ M	order (H_2O_2)[b]	order (H^+)[c]
0.24	0.67 ± 0.05	−1.42 ± 0.04
0.48	0.76 ± 0.04	−1.47 ± 0.10
0.72	0.84 ± 0.05	−1.38 ± 0.07
0.97	0.87 ± 0.04	−1.28 ± 0.05
1.21	0.86 ± 0.04	−1.33 ± 0.07
1.45	0.89 ± 0.02	−1.34 ± 0.07
1.69	0.89 ± 0.02	−1.33 ± 0.08
1.93	0.90 ± 0.02	−1.32 ± 0.08
2.17	0.93 ± 0.02	−1.28 ± 0.06
2.41	0.94 ± 0.01	−1.30 ± 0.06

[a] The uncertainties are the corresponding standard deviations. [b] $[H_2O_2]_0 = 0.0979-0.489$ M; $[HNO_3] = 2.31 \times 10^{-2}$ M; $T = 25.0$ °C. [c] $[H_2O_2]_0 = 0.294$ M; $[HNO_3] = 0.0231-0.102$ M; $[KNO_3] = 0.102$ M − $[HNO_3]$; $T = 25.0$ °C.

Apparent orders for Fe^{3+}, H_2O_2, and H^+ were obtained from the slopes of double-logarithm plots of the initial rate against the concentrations of those species. The values obtained for the apparent order of Fe^{3+} under a variety of experimental conditions were in the range 1.00−1.26, and they increased with increasing $[H_2O_2]_0$, increasing $[H^+]$, increasing ionic strength, and decreasing temperature (see Supporting Information). The values of the apparent orders of H_2O_2 and H^+ were obtained at different catalyst concentrations (Table 1). The apparent order of H_2O_2 was in the range 0.67−0.94, and it increased with increasing $[Fe^{3+}]$. The apparent order of H^+ was negative with absolute values in the range 1.28−1.47 that decreased with increasing $[Fe^{3+}]$.

Kinetic Data. From regression fits to the experimental data, it follows that the dependence of the initial rate on the catalyst concentration can be described by the equation

$$v_0 = \frac{a[Fe^{3+}]^{3/2}}{(1 + b[Fe^{3+}])^{1/2}} \quad (5)$$

which can be linearized as

$$\frac{[Fe^{3+}]^3}{v_0^2} = \frac{1}{a^2} + \frac{b}{a^2}[Fe^{3+}] \quad (6)$$

Under most experimental conditions, the $[Fe^{3+}]^3/v_0^2$ vs $[Fe^{3+}]$ plots were linear. In fact, of the 17 plots analyzed (at different values of $[H_2O_2]_0$, $[H^+]$, ionic strength, and temperature), 15 showed an excellent linearity and only 2 showed a slight upward-concave curvature. The latter two exceptions corresponded to the experimental series with the lowest values of $[H_2O_2]_0$. Typical examples of both kinds of behavior are shown in Figure 3.

Parameters a and b could be obtained from the intercept and slope of eq 6. Although the experimental errors associated with parameter a, and especially with parameter b, were rather high, the a^2/b ratio could be obtained with much more accuracy. Parameter a and the ratio a^2/b increased with increasing $[H_2O_2]_0$, whereas parameter b decreased. The three magnitudes decreased with increasing $[H^+]$. Double-logarithm plots of a, b, and a^2/b against the initial hydrogen peroxide concentration (Figure 4) and against the hydrogen ion concentration (Figure 5) were linear. An increase of the ionic strength was unfavorable for the reaction, and plots of the logarithms of a, b, and a^2/b against $I^{1/2}/(1 + I^{1/2})$ were linear with negative slopes in the three cases (Figure 6). The three kinetic magnitudes fulfilled the Arrhenius

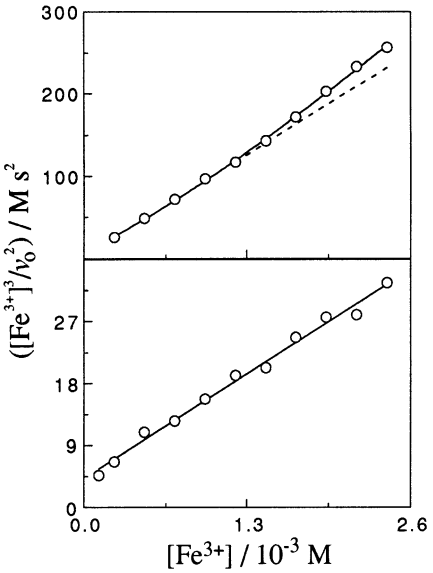

Figure 3. Dependence of the $[Fe^{3+}]^3/v_0^2$ ratio on the catalyst concentration for the iron(III)-catalyzed decomposition of H_2O_2 in the presence of HNO_3 (2.31×10^{-2} M) at 25.0 °C. $[H_2O_2]_0 = 9.79 \times 10^{-2}$ (top) and 0.294 (bottom) M. The dashed line represents the tangent to the curve at [catalyst] = 0.

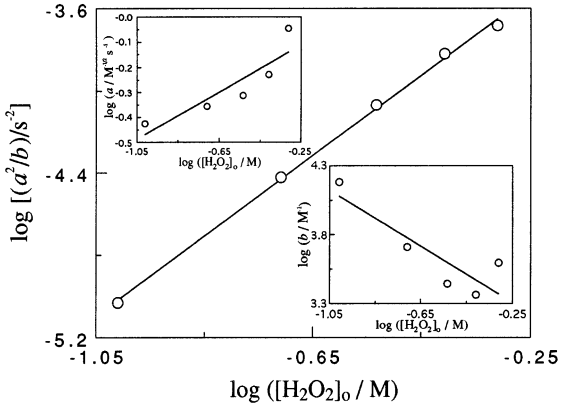

Figure 4. Double-logarithm plots of a^2/b (main figure), a (left inset), and b (right inset) against the initial hydrogen peroxide concentration for its decomposition catalyzed by Fe(III) [$(0.241-2.41) \times 10^{-3}$ M] in the presence of HNO_3 (2.31×10^{-2} M) at 25.0 °C.

law (Figure 7) with positive apparent activation energies in the three cases. The experimental data corresponding to the slopes of all these plots appear summarized in Table 2.

Rate Law. From these results, it follows that

$$a = k\frac{[H_2O_2]_0^{1/2}}{[H^+]^{3/2}} \tag{7}$$

$$b = \frac{k'}{[H_2O_2]_0[H^+]^{0.65}} \approx \frac{k'}{[H_2O_2]_0[H^+]} \tag{8}$$

$$\frac{a^2}{b} = \frac{k^2[H_2O_2]_0^2}{k'[H^+]^{2.48}} \approx \frac{k^2[H_2O_2]_0^2}{k'[H^+]^2} \tag{9}$$

The agreement of eqs 7−9 with the experimental data is excellent, except for the case of the dependencies of parameter

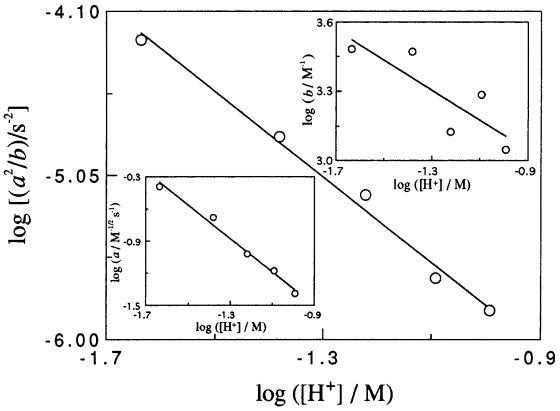

Figure 5. Double-logarithm plots of a^2/b (main figure), a (left inset), and b (right inset) against the hydrogen ion concentration for the decomposition of hydrogen peroxide (0.294 M) catalyzed by Fe(III) [$(0.241-2.41) \times 10^{-3}$ M] in the presence of HNO_3 at ionic strength 0.110 ± 0.007 M (KNO_3) and 25.0 °C.

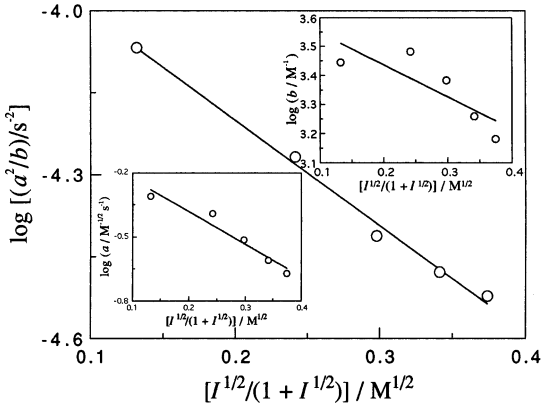

Figure 6. Dependence of parameters a^2/b (main figure), a (left inset), and b (right inset) on the ionic strength for the decomposition of hydrogen peroxide (0.294 M) catalyzed by Fe(III) [$(0.241-2.41) \times 10^{-3}$ M] in the presence of HNO_3 (2.31×10^{-2} M) and KNO_3 (0−0.334 M) at 25.0 °C.

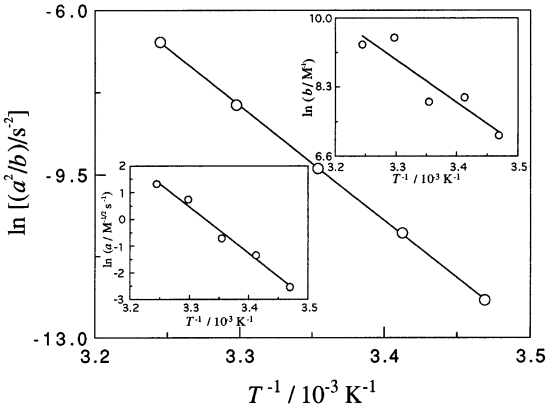

Figure 7. Arrhenius plots for parameters a^2/b (main figure), a (left inset), and b (right inset) for the decomposition of hydrogen peroxide (0.294 M) catalyzed by Fe(III) [$(0.241-2.41) \times 10^{-3}$ M] in the presence of HNO_3 (2.31×10^{-2} M) at 15.1−35.0 °C.

b and the ratio a^2/b on [H^+]. The experimental value of the slope of the log b vs log [H^+] plot (-0.65 ± 0.25) was slightly less negative than that expected from eq 8 (rounded to -1). Accordingly, the experimental value of the slope of the log a^2/b vs log [H^+] plot (-2.48 ± 0.15) was somehow more negative than that expected from eq 9 (rounded to -2).

TABLE 2: Experimental Data Associated with Each Kinetic Parameter[a]

data	*a*	*b*	a^2/b
slope (H_2O_2)[b]	0.47 ± 0.14	-1.01 ± 0.33	1.96 ± 0.05
slope (H^+)[c]	-1.56 ± 0.11	-0.65 ± 0.25	-2.48 ± 0.15
slope (I), $M^{-1/2d}$	-1.52 ± 0.21	-1.10 ± 0.43	-1.93 ± 0.09
E_a, kJ mol^{-1e}	146 ± 10	88 ± 21	203 ± 1

[a] The uncertainties are the corresponding standard deviations. [b] Slopes of log(parameter) vs log $[H_2O_2]_0$ linear plots. [c] Slopes of log(parameter) vs log $[H^+]$ linear plots. [d] Slopes of log(parameter) vs $I^{1/2}/(1 + I^{1/2})$ linear plots. [e] Apparent activation energies.

By substitution of eqs 7 and 8 in eq 5, we obtain the rate law:

$$v_0 = \frac{k\dfrac{[Fe^{3+}]^{3/2}[H_2O_2]_0^{1/2}}{[H^+]^{3/2}}}{\left(1 + k'\dfrac{[Fe^{3+}]}{[H_2O_2]_0[H^+]}\right)^{1/2}} \qquad (10)$$

which is also in excellent agreement with the experimental values found for the apparent kinetic orders. Effectively, according to eq 10, the apparent order of the catalyst must vary within the range $1 <$ order $(Fe^{3+}) < {}^3/_2$, increasing as either $[H_2O_2]_0$ or $[H^+]$ increases, as the ionic strength increases, or as the temperature decreases (the latter two cases due to the decrease of the experimental rate constant k'; see Supporting Information). On the other hand, the apparent order of the reactant must vary within the range ${}^1/_2 <$ order $(H_2O_2) < 1$ and increase as $[Fe^{3+}]$ increases, whereas the order of hydrogen ion must vary within the range $-{}^3/_2 <$ order $(H^+) < -1$, and its absolute value must decrease as $[Fe^{3+}]$ increases (see Table 1). The values obtained for the experimental rate constants were $k = (3.7 \pm 0.6) \times 10^{-3}$ $M^{1/2}$ s^{-1} and $k' = 28 \pm 11$ M (at ionic strength 3.11×10^{-2} M and 25.0 °C). However, it should be mentioned that the experimental data support fractional (rather than integral) orders for $[H^+]$ in eqs 8 and 9 and that eq 10 is thus approximate.

On the other hand, eq 10 reduces to eq 1 at high values of the $[Fe^{3+}]/[H_2O_2]_0[H^+]$ ratio (with $k_s = k/k'^{1/2}$). Moreover, eq 10 can also explain the finding that, at high values of $[Fe^{3+}]$, the ln $[H_2O_2]$ vs t plots showed a good linearity (see Figure 1, inset), since under those conditions the reaction becomes pseudo-first-order in H_2O_2.

Discussion

Mechanism. The involvement of fractional exponents in the experimental rate law (eq 10) strongly suggests that the Fe(III)−H_2O_2 reaction occurs through a radical-chain mechanism, since it would hardly fit a different kind of mechanism. The one that can be proposed to explain the experimental data found in the present work consists of the following steps:

$$Fe^{3+} + H_2O_2 \overset{K_I}{\rightleftharpoons} FeOOH^{2+} + H^+ \qquad (11)$$

$$FeOOH^{2+} \xrightarrow[\text{slow}]{k_{II}} Fe^{2+} + HO_2^{\bullet} \qquad (12)$$

$$Fe^{2+} + H_2O_2 \xrightarrow{k_{III}} Fe^{3+} + HO^- + HO^{\bullet} \qquad (13)$$

$$HO^{\bullet} + H_2O_2 \xrightarrow{k_{IV}} H_2O + HO_2^{\bullet} \qquad (14)$$

$$HO_2^{\bullet} \overset{K_V}{\rightleftharpoons} H^+ + O_2^{\bullet -} \qquad (15)$$

$$O_2^{\bullet -} + Fe^{3+} \xrightarrow{k_{VI}} O_2 + Fe^{2+} \qquad (16)$$

$$2HO_2^{\bullet} \xrightarrow{k_{VII}} H_2O_2 + O_2 \qquad (17)$$

$$Fe^{2+} + HO_2^{\bullet} \xrightarrow{k_{VIII}} Fe^{3+} + HO_2^- \qquad (18)$$

Equation 12 constitutes the chain-initiation step and eqs 13−16 the cyclic chain-propagation steps (addition of eqs 13−16 yields the global stoichiometry, eq 2), whereas two different chain-termination steps (eqs 17 and 18) are proposed. The value reported for the pK_a of the $HO_2^{\bullet}$ radical is 4.69.[29] This means that, under the experimental conditions of this work (pH 0.99−1.64), the equilibrium corresponding to eq 15 was shifted toward the left side with the acidic form of superoxide radicals ($HO_2^{\bullet}$) predominating over its basic form ($O_2^{\bullet -}$). In proposing the mechanism, I have considered that, although superoxide radicals are known to possess both oxidizing and reducing properties (they can disproportionate, as in eq 17), given that protonation results in a decrease of the electron density, of the two chemical forms of those radicals, $HO_2^{\bullet}$ is expected to be the better oxidant and $O_2^{\bullet -}$ the better reductant. Accordingly, I have proposed that $O_2^{\bullet -}$ is the species involved in the reduction of Fe^{3+} (eq 16), whereas $HO_2^{\bullet}$ is the species involved in the oxidation of Fe^{2+} (eq 18).

The mechanism proposed follows the basic scheme proposed by other authors for the Fe(III)−H_2O_2 and Fe(II)−H_2O_2 reactions. In particular, eqs 13 and 14 are consistent with the proposal by Haber and Weiss.[30] On the other hand, eqs 13, 14, and 18 are consistent with the proposal by Barb et al., although in their first proposal these authors assumed that Fe^{3+} was reduced by undissociated $HO_2^{\bullet}$.[31] However, Weiss and Humphrey interpreted the pH-dependence of the reaction rates assuming that Fe^{3+} was actually reduced by $O_2^{\bullet -}$ (as in eq 16),[32] and this interpretation was later accepted by Barb et al.[33] From pulse-radiolysis experiments, Rush and Bielski concluded that $HO_2^{\bullet}$ is capable of oxidizing Fe^{2+} ($k_{VIII} = 1.2 \times 10^6$ M^{-1} s^{-1}, eq 18) and that both $HO_2^{\bullet}$ and $O_2^{\bullet -}$ are capable of reducing Fe(III) complexes, although the anionic species is a much better reductant than the undissociated one, and the reactivity of each complex is rather independent of the ligand involved.[34] Taking from their work for the rate constant of the $Fe^{3+}-O_2^{\bullet -}$ reaction (eq 16) the value $k_{VI} = 1.5 \times 10^8$ M^{-1} s^{-1} and for that of the alternative $Fe^{3+}-HO_2^{\bullet}$ reaction the upper limit $k \leq 1 \times 10^3$ M^{-1} s^{-1} and taking for the pK_a of the $HO_2^{\bullet}$ radical the value 4.69,[29] we conclude that at pH 0.99−1.64 the rate of the $Fe^{3+}-O_2^{\bullet -}$ reaction (eq 16) is at least 30−134 times higher than that of the alternative $Fe^{3+}-HO_2^{\bullet}$ reaction. Thus, the results reported by Rush and Bielski are entirely consistent with the mechanism proposed in the present work. Although earlier works have reported values for the rate constant of the $Fe^{3+}-HO_2^{\bullet}$ reaction considerably higher,[35−39] the strong base catalysis found in the present work for the Fe(III)−H_2O_2 reaction suggests that the low value reported by Rush and Bielski might be more correct. It seems that those higher values might correspond to the reaction of Fe^{3+} with a mixture of $HO_2^{\bullet}$ and $O_2^{\bullet -}$ rather than with $HO_2^{\bullet}$ alone. Moreover, competition between the $Fe^{3+}-O_2^{\bullet -}$ and $Fe^{3+}-HO_2^{\bullet}$ reactions as chain-propagation steps cannot explain the acidity-related divergencies (fractional orders for

$[H^+]$ in eqs 8 and 9) found in the present work, given that the experimental data suggest more base catalysis than that expected from the proposed mechanism (not less, as would be the case if we include also the $Fe^{3+}-HO_2^{\bullet}$ reaction).

With respect to the chain-termination step corresponding to dismutation of superoxide radicals (eq 17), I have considered that, although the rate constant reported for the $HO_2^{\bullet}-O_2^{\bullet-}$ reaction ($k = 1.0 \times 10^8$ M^{-1} s^{-1}) is much higher than that reported for the $HO_2^{\bullet}-HO_2^{\bullet}$ reaction ($k_{VII} = 8.6 \times 10^5$ M^{-1} s^{-1}),[29] at the pH range of the present work the rate of the latter reaction was 10−43 times higher than that of the former.

The concentrations of the following intermediates can be deduced from the proposed mechanism by application of the steady-state approximation (see Supporting Information):

$$[Fe^{2+}] = \left(\frac{K_I k_{II}}{k_{III}}\right)^{1/2} \frac{K_V k_{VI}[Fe^{3+}]^{3/2}}{[H^+](K_V k_{VI} k_{VIII}[Fe^{3+}] + k_{III} k_{VII}[H_2O_2][H^+])^{1/2}} \quad (19)$$

$$[HO^{\bullet}] = \frac{(K_I k_{II} k_{III})^{1/2} K_V k_{VI}[Fe^{3+}]^{3/2}}{k_{IV}[H^+](K_V k_{VI} k_{VIII}[Fe^{3+}] + k_{III} k_{VII}[H_2O_2][H^+])^{1/2}} \quad (20)$$

$$[HO_2^{\bullet}] = \left(\frac{K_I k_{II} k_{III}[Fe^{3+}]}{K_V k_{VI} k_{VIII}[Fe^{3+}] + k_{III} k_{VII}[H_2O_2][H^+]}\right)^{1/2} [H_2O_2] \quad (21)$$

whereas those of $FeOOH^{2+}$ and $O_2^{\bullet-}$ can be easily deduced by application of the quasiequilibrium approximation to eqs 11 and 15, respectively. The law deduced from the proposed mechanism for the initial rate (Supporting Information, eq 32) is identical to the experimental one (eq 10) with

$$k = \left(\frac{K_I k_{II}}{k_{VII}}\right)^{1/2} K_V k_{VI} \quad (22)$$

$$k' = \frac{K_V k_{VI} k_{VIII}}{k_{III} k_{VII}} \quad (23)$$

$$\frac{k^2}{k'} = \frac{K_I k_{II} k_{III} K_V k_{VI}}{k_{VIII}} \quad (24)$$

The proposed mechanism is also in agreement with the effect of the ionic strength on the experimental parameters a and b and on the ratio a^2/b (see Table 2). This effect can be easily explained considering that eq 16 is the reaction between two unlike-charged ions ($O_2^{\bullet-}$ and Fe^{3+}), so an increase of the ionic strength results in a decrease of its associated rate constant (k_{VI}) and in a decrease of the experimental rate constants k and k' and of the ratio k^2/k' (see eqs 22−24) and also in a decrease of the experimental parameters a and b and of the ratio a^2/b (see eqs 7−9). Given the high electrostatic charge of one of the ions involved in that reaction (Fe^{3+}), the effect of the ionic strength on the value of rate constant k_{VI} is expected to be more important than its effect on other parameters also sensitive to the ionic strength (equilibrium constants K_I and K_V). Whereas K_I is expected to decrease with increasing ionic strength (the reverse reaction of eq 11 involves two like-charged ions), K_V is expected to increase (the reverse reaction of eq 15 involves two unlike-charged ions). This would explain the finding that the experimental rate constant k is more affected by the ionic strength than rate constant k' and that the ratio k^2/k' is the most affected of the three, since whereas rate constant k depends on both equilibrium constants K_I and K_V, rate constant k' depends only on equilibrium constant K_V. This means that the decrease of rate constant k_{VI} with increasing ionic strength is partially compensated by the increase of equilibrium constant K_V in the three cases (see eqs 22−24) but that decrease is reinforced by the parallel decrease of equilibrium constant K_I only in the cases of the experimental rate constant k (directly proportional to the square root of K_I) and the ratio k^2/k' (directly proportional to K_I).

The apparent activation energy associated with the experimental rate constant k (146 ± 10 kJ mol^{-1}) is higher than that associated with rate constant k' (88 ± 21 kJ mol^{-1}), and the apparent activation energy associated with the ratio k^2/k' (203 ± 1 kJ mol^{-1}) is the highest of the three. These values correlate very well with the excess in the number of rate constants in the numerators of eqs 22−24 with respect to the corresponding denominators, since that excess is 0 for the experimental rate constant k' (lowest apparent activation energy), 1 for rate constant k (intermediary activation energy), and 2 for the ratio k^2/k' (highest activation energy). The equilibrium constants K_I and K_V have not been considered, since the absolute values of their associated reaction enthalpies ($\Delta H°$) are expected to be lower than the activation energies (E_a) associated with the rate constants corresponding to the elementary steps.

Acidity-Related Divergencies. The predictions of the proposed mechanism on the dependencies of the initial rate on $[Fe^{3+}]$ and $[H_2O_2]_0$ are in excellent agreement with the experimental data. However, its predictions with respect to the dependency on $[H^+]$ are excellent only for the experimental parameter a and a little worse for parameter b and the ratio a^2/b. Whereas, according to the proposed mechanism, the slope of the log b vs log $[H^+]$ and log(a^2/b) vs log $[H^+]$ plots should be -1 and -2, respectively, the corresponding experimental values are -0.65 ± 0.25 and -2.48 ± 0.15. This divergency could be explained if we accept the existence of two additional steps:

$$Fe^{2+} + H_2O \overset{K_{IX}}{\rightleftharpoons} FeOH^+ + H^+ \quad (25)$$

$$FeOH^+ + H_2O_2 \xrightarrow{k_X} FeOH^{2+} + HO^- + HO^{\bullet} \quad (26)$$

The value reported for the equilibrium constant associated with eq 25 is $K_{IX} = [FeOH^+][H^+]/[Fe^{2+}] = 5.0 \times 10^{-4}$ M [at ionic strength 1 M ($NaClO_4$) and 25.0 °C], whereas that associated with the corresponding equilibrium for the oxidized form of the catalyst is $K = [FeOH^{2+}][H^+]/[Fe^{3+}] = 1.0 \times 10^{-3}$ M [at ionic strength 3 M ($NaClO_4$) and 25.0 °C].[40] Thus, under the acidic conditions of this work (pH 0.99−1.64), the equilibria associated with eq 25 and with the corresponding reaction for Fe(III) would both be shifted to the left side with the complexes $FeOH^+$ and $FeOH^{2+}$ in very low concentration ($[FeOH^+]/[Fe^{2+}] = 4.9 \times 10^{-3}$ to 2.2×10^{-2}, $[FeOH^{2+}]/[Fe^{3+}] = 9.8 \times 10^{-3}$ to 4.4×10^{-2}). However, considering that substitution of a water molecule by a hydroxyl ion in the coordination spheres of Fe(II) and Fe(III) would result in an increase of their electron densities and, thus, in an increase of the reducing power of Fe(II) and a decrease of the oxidizing power of Fe(III), the value of rate constant k_X could be high enough for eq 26 to compete with eq 13, although the contribution of $FeOH^{2+}-H_2O_2$ reaction as an alternative to eq 11 under the acidic conditions of the present work is probably small enough to be neglected.

The expressions for the experimental parameters would then be (see Supporting Information)

$$a = \left(\frac{K_I k_{II}}{k_{VII}}\right)^{1/2} K_V k_{VI} \frac{[H_2O_2]_0^{1/2}}{[H^+]^{3/2}} \quad (27)$$

$$b = \frac{K_V k_{VI} k_{VIII}}{(k_{III}[H^+] + K_{IX}k_X)k_{VII}[H_2O_2]_0} \quad (28)$$

$$\frac{a^2}{b} = \frac{K_I k_{II}(k_{III}[H^+] + K_{IX}k_X)K_V k_{VI}}{k_{VIII}} \frac{[H_2O_2]_0^2}{[H^+]^3} \quad (29)$$

We can see that eqs 27−29 are in perfect agreement with the experimental data (Table 2) as far as the dependency on $[H_2O_2]_0$ is concerned and eq 27 also as far as the dependency on $[H^+]$ is concerned. On the other hand, for relatively narrow ranges of $[H^+]$ as the one used in this study (0.02−0.10 M), eqs 28 and 29 predict that the double-logarithm plots of b and a^2/b vs $[H^+]$ will be roughly linear with slopes within the ranges $-1 <$ slope (b) < 0 and $-3 <$ slope (a^2/b) < -2, also in agreement with the experimental data.

Chain-Termination Steps. Of the 17 $[Fe^{3+}]^3/v_0^2$ vs $[Fe^{3+}]$ plots analyzed, 15 showed an excellent linearity (see Figure 3, bottom), in agreement with the proposed mechanism. However, the two plots corresponding to low values of $[H_2O_2]_0$ showed a slight upward-concave curvature (see Figure 3, top). This divergency can also be accounted for considering an additional chain-termination step:

$$Fe^{2+} + HO^\bullet \xrightarrow{k_{XI}} Fe^{3+} + HO^- \quad (30)$$

that is consistent with one of the elementary reactions in the mechanism proposed by Barb et al.[33]

From eqs 19−21, it follows that for a given value of $[Fe^{3+}]$ the concentrations of the intermediates Fe^{2+} and $HO^\bullet$ decrease as $[H_2O_2]_0$ increases, whereas that of $HO_2^\bullet$ increases. On the other hand, for a given value of $[H_2O_2]_0$, the concentrations of the three intermediates increase as $[Fe^{3+}]$ increases, but those of Fe^{2+} and $HO^\bullet$ increase much more than that of $HO_2^\bullet$. Hence, at high values of the $[H_2O_2]_0/[Fe^{3+}]$ ratio the predominant chain-termination step is expected to be eq 17, but at moderate values of that ratio eq 18 will predominate, and at low values, eq 30 will be the predominant chain-termination step. Under the latter conditions, the mechanism would be given by eqs 11−16 and 30, leading to the following rate law (see Supporting Information):

$$v_0 = \frac{K_I k_{II}[Fe^{3+}][H_2O_2]_0}{[H^+]} + \left(\frac{K_I k_{II} k_{III} k_{IV}}{k_{XI}}\right)^{1/2} \frac{[Fe^{3+}]^{1/2}[H_2O_2]_0^{3/2}}{[H^+]^{1/2}} \quad (31)$$

Therefore, as the $[H_2O_2]_0/[Fe^{3+}]$ ratio decreases the rate law should change progressively from eq 10 to eq 31. This means that at low values of $[H_2O_2]_0$ and high values of $[Fe^{3+}]$ the apparent kinetic order of Fe^{3+} should decrease with respect to the value predicted by eq 10 ($1 <$ order $< {}^3/_2$) to approach that predicted by eq 31 (${}^1/_2 <$ order < 1), which explains the upward-concave curvature of the $[Fe^{3+}]^3/v_0^2$ vs $[Fe^{3+}]$ plots observed under those conditions (see Figure 3, top). Moreover, eq 31 is consistent with the apparent kinetic order >1 for H_2O_2 reported by some authors for kinetic experiments with extremely low values of that ratio ($[H_2O_2]_0/[Fe^{3+}] = 0.002-1.0$).[21,41]

However, under the experimental conditions of the present work, where much higher values for that ratio were used ($[H_2O_2]_0/[Fe^{3+}] = 41-2028$), the contribution of eq 30 as chain-termination step would be very minor, so the mechanism would be given essentially by eqs 11−18.

Supporting Information Available: Apparent kinetic orders of iron(III); derivation of the rate law, (i) high peroxide/catalyst ratio—basic mechanism, (ii) high peroxide/catalyst ratio—extended mechanism, and (iii) low peroxide/catalyst ratio. This material is available free of charge via the Internet at http://pubs.acs.org.

References and Notes

(1) Johnson, G. R. A.; Nazhat, N. B.; Saadalla-Nazhat, R. A. *J. Chem. Soc., Chem. Commun.* **1985**, 407.
(2) Masarwa, M.; Cohen, H.; Meyerstein, D.; Hickman, D. L.; Bakac, A.; Espenson, J. H. *J. Am. Chem. Soc.* **1988**, *110*, 4293.
(3) Mohamadin, A. M. *J. Inorg. Biochem.* **2001**, *84*, 97.
(4) Halliwell, B.; Gutteridge, J. M. C. *Methods Enzymol.* **1990**, *186*, 1.
(5) Slyshenkov, V. S.; Moiseenok, A. G.; Wojtczak, L. *Free Radic. Biol. Med.* **1996**, *20*, 793.
(6) Rojkind, M.; Dominguez-Rosales, J. A.; Nieto, N.; Greenwel, P. *Cell. Mol. Life Sci.* **2002**, *59*, 1872.
(7) Rush, J. D.; Koppenol, W. H. *J. Biol. Chem.* **1986**, *261*, 6730.
(8) Rush, J. D.; Koppenol, W. H. *J. Inorg. Biochem.* **1987**, *29*, 199.
(9) Rahhal, S.; Richter, H. W. *J. Am. Chem. Soc.* **1988**, *110*, 3126.
(10) Yamazaki, I.; Piette, L. H. *J. Am. Chem. Soc.* **1991**, *113*, 7588.
(11) Sawyer, D. T.; Kang, C.; Llobet, A.; Redman, C. *J. Am. Chem. Soc.* **1993**, *115*, 5817.
(12) Hage, J. P.; Llobet, A.; Sawyer, D. T. *Bioorg. Med. Chem.* **1995**, *3*, 1383.
(13) Sawyer, D. T.; Sobkowiak, A.; Matsushita, T. *Acc. Chem. Res.* **1996**, *29*, 409.
(14) Walling, C. *Acc. Chem. Res.* **1998**, *31*, 155.
(15) MacFaul, P. A.; Wayner, D. D. M.; Ingold, K. U. *Acc. Chem. Res.* **1998**, *31*, 159.
(16) Goldstein, S.; Meyerstein, D. *Acc. Chem. Res.* **1999**, *32*, 547.
(17) Kremer, M. L. *Phys. Chem. Chem. Phys.* **1999**, *1*, 3595.
(18) Marusawa, H.; Ichikawa, K.; Narita, N.; Murakami, H.; Ito, K.; Tezuka, T. *Bioorg. Med. Chem.* **2002**, *10*, 2283.
(19) Kremer, M. L. *J. Phys. Chem. A* **2003**, *107*, 1734.
(20) Edwards, J. O.; Curci, R. In *Catalytic Oxidations with Hydrogen Peroxide as Oxidant*; Strukul, G., Ed.; Kluwer: Dordrecht, The Netherlands, 1992; p 98.
(21) Barb, W. G.; Baxendale, J. H.; George, P.; Hargrave, K. R. *Trans. Faraday Soc.* **1951**, *47*, 591.
(22) Walling, C.; Goosen, A. *J. Am. Chem. Soc.* **1973**, *95*, 2987.
(23) Kremer, M. L.; Stein, G. *Trans. Faraday Soc.* **1959**, *55*, 959.
(24) Kremer, M. L. *Trans. Faraday Soc.* **1963**, *59*, 2535.
(25) Brown, S. B.; Jones, P.; Suggett, A. *Prog. Inorg. Chem.* **1970**, *13*, 159.
(26) Baxendale, J. H. *Adv. Catal.* **1952**, *4*, 31.
(27) Lewis, T. J.; Richards, D. H.; Salter, D. A. *J. Chem. Soc.* **1963**, 2434.
(28) Jeffery, G. H.; Bassett, J.; Mendham, J.; Denney, R. C. *Vogel's Quantitative Chemical Analysis*; Longman: Essex, U.K., 1991; p 372.
(29) Sawyer, D. T.; Valentine, J. S. *Acc. Chem. Res.* **1981**, *14*, 393.
(30) Haber, F.; Weiss, J. *Proc. R. Soc. London, Ser. A* **1934**, *147*, 332.
(31) Barb, W. G.; Baxendale, J. H.; George, P.; Hargrave, K. R. *Nature* **1949**, *163*, 692.
(32) Weiss, J.; Humphrey, C. W. *Nature* **1949**, *163*, 691.
(33) Barb, W. G.; Baxendale, J. H.; George, P.; Hargrave, K. R. *Trans. Faraday Soc.* **1951**, *47*, 462.
(34) Rush, J. D.; Bielski, B. H. J. *J. Phys. Chem.* **1985**, *89*, 5062.
(35) Allen, A. O.; Hogan, V. D.; Rothschild, W. G. *Radiat. Res.* **1957**, *7*, 603.
(36) Rothschild, W. G.; Allen, A. O. *Radiat. Res.* **1958**, *8*, 101.
(37) Dobson, G.; Hughes, G. *Trans. Faraday Soc.* **1961**, *57*, 1117.
(38) Pucheault, J.; Ferradini, C.; Buu, A. *Int. J. Radiat. Phys. Chem.* **1969**, *1*, 209.
(39) Sehested, K.; Bjergbakke, E.; Rasmussen, O. L.; Fricke, H. *J. Chem. Phys.* **1969**, *51*, 3159.
(40) Sillen, L. G. *Stability Constants of Metal-Ion Complexes*; The Chemical Society: London, 1971; Supplement No. 1, p 22.
(41) Andersen, V. S. *Acta Chem. Scand.* **1950**, *4*, 914.